Vital Role of Water Flow and Moisture Distributionin Soils and the Necessity of a New Out-Look and Simulation Modeling of Soil- Water Relations

Mostafa H. Hilal[1] and Nabil M. Anwar[2]

[1]National Research Centre, Cairo, Egypt
[2]National water Research Centre., Egypt
mostafa@gizatec.com, nabilmanwar@hotmail.com

Abstract: Irrigation is the process of adding water to a soil to compensate for water losses by deep percolation, drainage, seepage, evaporation, transpiration and plant uptake. Moreover, downward movement of water through a soil profile, transports salts and nutrients deeper in the soil profile, while moisture and nutrients are retained in the micropores for the benefit of plants. Water flow and moisture movement in soils occur under 3 successive steps which are reflected on movement and residence of water, nutrients and salts as follows: 1) Intake of irrigation water by dry soil, 2) Soil Water flow from saturated layer to drier layer below field capacity, and 3) Water flow above saturation (under positive head). Water flow and moisture distribution in soil pores are governed by several important factors: 1) Irrigation frequency and scheduling. 2) Soil stratification. 3) Magnetization of irrigation water. 4) Control of soil salinity and alkalinity by treating soils with "Nile Fertile" which is a water absorber and an acid producer. Modeling water flow in unsaturated soils is very important for understanding many processes that occur in the plant-soil-water system. Many mathematical models simulate water flow in unsaturated soils using Richards' Equation, while other models use analytical or semi-analytical solutions based on such equation. Richards' Equation considers the soil as a system of a large number of small tubes that vary in diameter from very fine capillary micropores to larger gravitational macropores. It assumes that a soil segment sucks in water by the same suction head used to suck out water from it. It also assumes that water follows the same path in the soil during wetting but in the opposite direction as compared to drying. Richards' equation is highly non-linear and requires the numerical solution to use very small spatial and temporal increments. However, the soil behavior is 'hysteretic' with respect to many phenomena such as sorption and desorption of heavy metals, magnetization and demagnetization of adsorbed water, and wetting and drying. The objective of this work was to provide a new understanding for water flow equations in the soil, where water flow is direction-dependent. Infiltration rate at the soil surface was obtained using relations of Eagleson and Phillip. Thereafter, Green-Ampt model was rearranged to obtain suction head at the wetting front using the infiltration rate as defined by Eagleson. Suction head at the wetting front was used to develop a new curve for sorption suction head at all water contents. The obtained curve is used instead of the pF curve in solving Richards' Equation during sorption. This is because; water and moisture flow in the soil is directional. Besides, downward flow differs from upward flow. Rate of downward flow is estimated using the new sorption suction head curve, with the condition of no flow leaving the soil segment until the micropores are filled with water (reach field capacity). On the other hand, upward flow is solved using the pF curve as in Richards' Equation solution. Simulation results of this work during ponded infiltration showed more infiltration water entering into the profile that penetrated deeper as compared to Richards' Equation solution. Redistribution following the end of infiltration showed faster gravitational flow in the upper part of the profile above field capacity as compared to the solution of Richards' Equation, and the drained water was absorbed in the next segment of the profile. This work will make numerical solution of water flow in unsaturated soil layers not need small spatial and temporal increments for wetting and drying processes.

[Mostafa H. Hilal and Nabil M. Anwar. **Vital Role of Water Flow and Moisture Distribution in Soils and the Necessity of a New Out-Look and Simulation Modeling of Soil- Water Relations.** *J Am Sci* 2016;12(7):6-18]. ISSN 1545-1003 (print); ISSN 2375-7264 (online). http://www.jofamericanscience.org. 2. doi:10.7537/marsjas120716.02.

Key words: Soil stratification, water magnetization, frequency of irrigation, sorption-desorption suction head, infiltration rate, Nile Fertile.

1. Introduction

Importance of water flow in soils and difficulties of characterization:

Wetting process of a dry soil:

Irrigation is the process of adding water to a soil to compensate for water losses by evaporation, transpiration, deep percolation, drainage and/or seepage. Water flowing down in the soil dissolves nutrients and salts and allows for exchange of Oxygen and CO_2 between the soil water and soil air. Anwar and Hilal (2015) indicated that increasing water flow leached NaCl out of the soil profile faster, while other

salts such as Mg and K salts were retained in the soil. It also stores nutrients and dissolved salts within the soil matrix, and transports them to the plant roots.

Moreover, downward movement of water through the profile, transports salts and nutrients deeper in the soil profile. Water flow and moisture movement in soils occur under 3successive steps which are reflected on movement and residence of water, nutrients and salts as follows:

1) Intake of irrigation water by dry soil, when water is added to dry soil, it infiltrates stepwise down through larger gravitational pores, then it is simultaneously adsorbed by finer pores forming a wetting front, until the soil reaches field capacity.

2) Soil Water flow from saturated layer to drier layer below field capacity, Water moves through larger gravitational pores down the profile (*Nile Fertile is a bio-mineral sulfur fertilizer mixture; produced by Giza Tec Co., October City, Egypt*) to drier soil below, where micro-pores are already filled.

3) Water flow above saturation (under positive head),Above saturation, excess water addition forms a water head which displaces soil water and pushes it down towards water table. Extra water addition in open field forms a pond, which flows as run-off down a slope or towards an open drain.

Water flow and moisture distribution in soil pores are governed by several important factors (Hilal 2015):

1. Irrigation frequency and scheduling.
2. Soil stratification.
3. Magnetization of irrigation water.
4. Control of soil salinity and alkalinity by treating soils with **"Nile Fertile"** which is a water absorber and an acid producer.

Effect of irrigation frequency on water consumption by evaporation and by transpiration, in a cotton field:

Comparing the efficiency of irrigation frequency of Egyptian cotton, grown in a clay loam soil in the south of Nile Delta, indicated that water loss by evaporation was 60% less in case of irrigation every two weeks as compared to irrigation once every week. However, transpiration was unaffected and was similar in the two cases of irrigation.Thus, such cutout of evaporation loss leads to much better irrigation efficiency, (Hilal 2015).

Effect of soil stratificationon water and salt transport in soil- columns.

When using high salinity water in irrigation, large quantities of salts are consequently applied to the soil surface. Some of these salts dissolve completely or partially in the soil solution, thus acceptable to transport through the profile. The major parameters that influence salt transport in the soil are hydraulic conductivity, moisture and solute retention and micropore/macropore balance (Hilal et al 1997).

They studied the effect of inducing a gravel layer in a sandy soil column, on salt accumulation on the top 3 cm. In homogenous soil columns, EC increased by incubation from 15 to 22dS/m, after 120 days of wetting and drying. While in stratified columns EC values of the top layers were far lower, ranging from 11.0 to 14.5 dS/m. The increase of salt accumulation in homogenous soil was most probably due to capillary continuity and evaporation. Induced gravel layer cut the capillary rise and acts as an evaporation barrier.

Magnetic treatment of irrigation water:

Investigation of magnetic field effects on soils and plants, started more than 50 years ago. However, the concept of using magnetized water and solutions is relatively recent.

In an olive farm irrigated with moderately saline water through a drip system of irrigation: analysis, of different soil layers ahead and beyond the placement of a magnetic unit, were conducted. Magnetized irrigation water was shown to have three main functions:

(1) Increasing the leaching of excess soluble salts (2) Lowering soil alkalinity; (3) Disolving slightly soluble salts such as carbonates, phosphates and sulfates.

Such effects were also demonstrated by **Hilal and Helal (2000)** in a citrus orchard where the solubility and uptake of Ca^{+2}, Mg^{+2} and SO^{2-}_4 were accelerated while Na^{+} uptake was reduced to one half by magnetized water.

Nile Fertile for using saline water for irrigation in coastal zones:

Soil columns experiments, under the conditions of the North Coast of Egypt, were conducted to grow wheat using Sea water or highly saline well water for subsurface complementary irrigation. Natural shallow saline water table or subsurface irrigation with sea water to maintain a saline water table, at 60 to 65 cm below the surface, proved to greatly promote wheat production. When, a complementary irrigation with non saline water was conducted, NF initiated good wheat growth and yield, even better than multiple irrigations with non saline water (where water table is relatively deep).

An empirical model, that suites wheat production in certain coastal area was developed by Hilal and Kotb, as reported by (Hilal 2015). Obtained Data, indicated considerable promotion effects of NF application on wheat. In rainy arias without complementary irrigation, where shallow saline water table is dominant, NF increased wheat growth 4 folds as compared to the traditional NPK fertilizers.

It is known that capillary pores have the power to pull water upward from the shallow saline water table, leaving salts down. Continuous upward movement of moisture from the water table or from a saturated layer, below the surface, to the root zone or to the soil surface is sustained by evaporation and / or evapotranspiration.

Modeling water flow in unsaturated soils is very important for understanding many processes that occur in the plant-soil-water system. Different irrigation systems allow for variable rates of water movement and distribution in the soil, which cause more variability in other processes in soil-water system. Successful description of water movement models for flow mechanism and characterization of soil water system will make it useful to use the calculated water fluxes and water contents in modeling the transport of salts and nutrients. Many Models simulate unsaturated soil water flow based on one-dimensional highly non-linear Richards' Equation:

$$\frac{\partial \boldsymbol{\theta}}{\partial t} = \frac{\partial}{\partial z}\left[\boldsymbol{k(\theta)}\frac{\partial h}{\partial z}\right] - \frac{\partial \boldsymbol{k(\theta\theta)}}{\partial z} \qquad \textbf{(1)}$$

where Θ is volumetric soil moisture content (cm^3/cm^3), h is soil water suction head (cm), z is vertical distance (cm) and k(Θ) is unsaturated hydraulic conductivity (cm/hr). Many others have used analytical solutions based on Richards' Equation under certain initial and boundary conditions (e.g. Szymkiewicz, 2004; van Genuchten et al., 1992). The non-linear equation is solved using the relation between the soil matric suction head and soil wetness (soil water characteristic curve; or pF curve), and the unsaturated hydraulic conductivity curve, together with the initial and boundary conditions. Numerical solution of this highly non-linear equation requires very small spatial and temporal increments with massive iterations.

Wetting of soil profile during ponded irrigation into dry soil is simulated by Richards' Equation assuming very high suction head gradient by difference between wet and dry soil gridpoints, together with the average hydraulic conductivity of wet and dry soil. It also assumes that fine pores suck in the infiltration water until they are filled, and thereafter larger size pores are filled, until the soil reaches saturation. Meanwhile, it also assumes that empty finer pores in the lower depth will then suck water from these pores, driven by difference in suction head gradient and antecedent hydraulic conductivity that increases as more pores are wetted. In contrary, water always follows the path of least resistance, which deviates from this theoretical description.

Drying of saturated soil

Evaporation from the surface soil triggers the process of drying. Connectivity of moisture in the micropores generates a continuous capillary flow that maintains the processes of evaporation and drying of the profile. An upward capillary movement is activated under the developed suction head gradient to compensate for the lost moisture. When the soil surface is dry, and is heated during the day, remaining moisture is vaporized, capillary flow is interrupted, and evaporation from soil surface stops. Condensation during the night and early morning hours fills the micropores of the soil surface, reconnects the soil micropores and restarts evaporation.

Stratification of the profile can also cause pore disconnectivity, interrupt capillary flow and stop evaporation and drying process. This can be used to protect soil water from evaporation losses and to maintain moisture around the plant roots between irrigations. A sandy layer on top of a clay profile will protect moisture in the clay from evaporation, where the plant roots vulnerability to drought stress between irrigations will be reduced. It is thus clear that downward water movement is mainly in the gravitational macropores, while upward movement is mainly in the capillary micropores. The phenomenon of following a different path in the reverse process is known as the process of Hysteresis.

Hysteresis

Elbana (2013), in a study for examining heavy metals behavior in soils, heavy metals exhibited strong nonlinear and kinetic retention behavior. Cd was nearly immobile in alkaline soils with 2.8% $CaCO_3$, whereas 20 and 30% of the applied Cd was mobile in the acidic soil and the subsurface layer of the alkaline soil with 1.2% $CaCO_3$, respectively. Moreover, in a field study of the spatial distributions of the accumulation of Cd among soil depths as consequence of irrigation with domestic wastewater, he found homogeneous retention within soil depths.

Soils are hysteretic with respect to some phenomena such as sorption and desorption of heavy metals. Cd sorption-desorption results for 3 soils indicate considerable hysteresis. This hysteretic behavior resulted from discrepancies between the adsorption and desorption isotherms, in view of kinetic retention behavior of Cd in these soils and is indicative of non equilibrium behavior of the retention mechanisms (Zhang and Selim, 2005).

Hilal, (2015) reported that Hysteretic behavior also exists in magnetization. His data presented in Figure (1) shows two different paths for magnetic effects: the first is what magnetic materials follow during magnetization; the second path is that of de-magnetization.

Water is a diamagnetic material that exhibit hysteretic behavior as well, while it maintains its magnetization for a short duration of about one day. Meanwhile, recording materials retain magnetism for several years.

Deviation of soil behavior during wetting and drying was reported by Hillel (1998) to cause what is known as Hysteresis that differs from behavior of Richards' Equation. Measurements and calculations indicated that, under using Richards' Equation, the relation between soil water suction head and soil water content in pF curve varies during wetting and drying and follows different paths depending on the initial water content at the beginning of each wetting event (Figure 2).

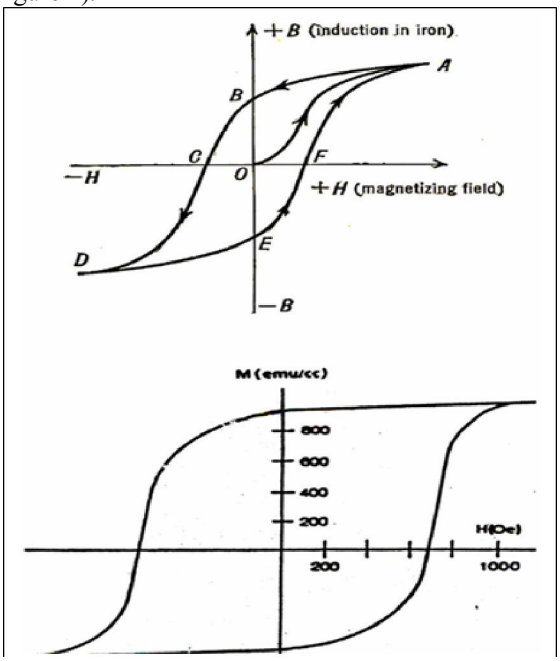

Figure (1): Hysteresis loop for a typical metallic Hysteresis curve for a magnetic recording material magnetization cycle

The relation between soil matrix suction head and soil wetness can be obtained in two ways:

(1) In desorption, by starting with a saturated sample and applying increasing suction, in a step-wise manner, to gradually dry the soil while taking successive measurements of wetness versus suction;

(2) In sorption, by gradually wetting an initially dry soil sample while reducing the suction stepwise (Hillel 1998). Each of these methods yields a curve, but the two curves will generally not be identical.

The equilibrium between suction heads and water contents are greater in desorption (drying) than in sorption (wetting). This dependence upon the direction of the process is called Hysteresis (Haines, 1930; Miller and Miller, 1955a & b, 1956; Philip, 1964; Topp and Miller, 1966; Bomba, 1968; Topp, 1969). As reported by Hillel (1998), hysteresis is attributed to several factors such as non-uniformity of individual pores, changes of contact angle during wetting and drying, and soil swelling, shrinking and air entrapment.

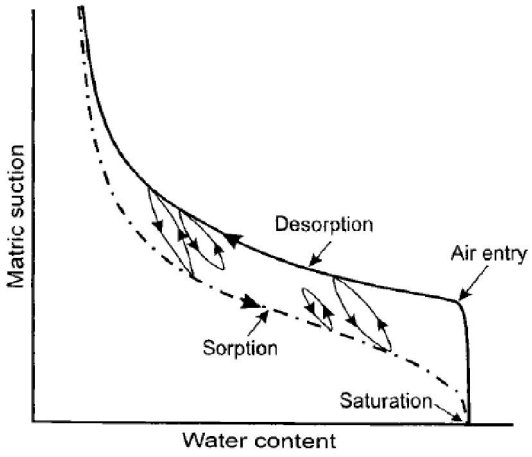

Figure (2): Soil matrix suction head vs. water content curves in sorption and desorption. The intermediate loops represent complete or partial transitions between the main wetting and drying curves, Quoted from Hillel (1998).

Most unsaturated flow models use the drying pF curve, and neglect the effects of hysteresis. Figure (2) shows the hysteretic relation between soil matric suction head and soil water content as it varies with different wetting and drying cycles. At a given water content, the soil will tend to exhibit greater suction in desorption than in sorption Hillel (1998).

Preferential macropore/micropore water flow

Hysteretic relation between suction head and water content is obtained using the resultant flow driven by hydraulic conductivity and average suction of micro and macropores. During infiltration, sorption suction head of dry soil is relatively high and most macropore water is sucked into micropores. As water advances to lower soil segment, sorption suction head goes lower and more water flows down the profile.

During vertical distribution that follows infiltration, macropore water that is held at relatively small suction head, flows downwards at the unsaturated macropore hydraulic conductivity under head gradient of gravity and difference of sorption suction with next layer in the profile. However, when water table rises, water flows upwards in the profile driven by the net head gradient of sorption suction that goes against gravity. This work estimates the sorption suction head curve at different soil water contents. This new curve is used for solving Darcy's Law when the soil undergoes sorption, while the drying pF curve is used in desorption.

Darcy's Law expresses water flux as:

$$\boldsymbol{q = K(\theta\Theta)\frac{\partial H}{\partial Z}} \qquad \textbf{(2)}$$

Where q is water flux (cm/hr), K (Θ) is unsaturated hydraulic conductivity (cm/hr), Θ is volumetric soil water content (cm^3/cm^3), H is total

head (H=h-z), h is soil matric suction head, and z is vertical distance.

Darcy's Law and Richards' Equation as expressed above, are related by the continuity equation:

$$\frac{\partial \theta \Theta}{\partial t} = \frac{\partial q}{\partial Z} \quad (3)$$

Water flow is dependent on direction; and Darcy's Law description for downward flow will differ from upward flow in this work. Downward flow will also differ in cases of ponded and non-ponded infiltration events. Combining equations 2 & 3 results in equation (1) mentioned above (Richards' Equation).

2. Methodology

Field and green house evaluations of factors, governing water flow and distribution in soils

Irrigation scheduling

A study was conducted to compare small-depth frequent irrigation as in center-pivot sprinkler and drip irrigation systems with larger-depth less frequent irrigation as in surface irrigation of field crops, maintaining the same total amount of irrigation water for all field plots.

Magnetic treated irrigation water

Four soil pots of 3 kg capacity each were irrigated with saline water taken from a well at RasSidre, having an E.C. value of 8.2 mmohs/cm. Two pots were irrigated with magnetized water using a magnetron of 1 inch diameter*, and the others were irrigated with normal saline water. Volume and salinity of leachates were determined.

Soil stratification

A laboratory experiment was conducted using 4 groups of plexi-glass columns, 10 cm in diameter and 40 cm long. A group of columns is homogeneous sandy soil. The second group of columns is filled with homogeneous sandy loam soil.

The third and fourth groups of columns were filled with two equal layers (15 cm depth): Sand over sandy loam and sandy loam over sand. The columns were treated with dilute NaCl solution of 2000 ppm concentration, and were covered for 2 days to achieve moisture equilibrium (preferably at field capacity), and then were left to dry for a drying period of one month. Remaining moisture and total dissolved salts in different layers of each soil column were then estimated.

Determination of Infiltration Rate:

1) Eagleson Infiltration Model

The downward flow (infiltration rate) is obtained using methodology of Eagleson (1978):

$$i \approx \frac{1}{2} S_i t^{-1/2} + \frac{1}{2}[K(\Theta_1) + K(\Theta_o)] \quad (4)$$

Where Θ_o and Θ_1 are the initial and final water contents, respectively, and S_i is the infiltration sorptivity, obtained by Eagles on (1978):

$$S_i = 2(\Theta_1 - \Theta_o)[D_i/\pi]^{1/2} \quad (5)$$

and D_i is the effective infiltration diffusivity over the range $\Theta_1 - \Theta_o$, which is approximated well by Crank (1956):

$$D_i = \frac{5}{3}(\Theta_1 - \Theta_o)^{-5/3} \int_{\Theta_o}^{\Theta_1} (\Theta_1 - \Theta_o)^{2/3} D(\Theta)\, d\Theta \quad (6)$$

where $D(\Theta)$ is the diffusivity:

$$D(\Theta) = k(\Theta) \frac{\partial h}{\partial \Theta} \quad (7)$$

Equations (10) and (11) are solved graphically in this work using the trapezoidal rule.

Unsaturated Hydraulic Conductivity

The unsaturated hydraulic conductivity is determined in this work by Millington and Quirk (1960):

$$K(\Theta_i) = K(\Theta_s) \left(\frac{\Theta_i}{\Theta_s}\right)^P \frac{\sum_{j=1}^{m} (2j+1-2i)/h_j^2}{\sum_{j=1}^{m} (2j-1)/h_j^2} \quad (8)$$

where $K(\Theta_i)$ is the calculated unsaturated hydraulic conductivity at water content Θ_i, $K(\Theta_s)$ is the saturated hydraulic conductivity, Θ_s is the water content at saturation, m is the number of increments used in the computation, i and j are indices, and p = 1 in most cases (Knuze et al. 1968; Jackson, 1972). Soil-water characteristic curve for the same soil is shown in figure (3).

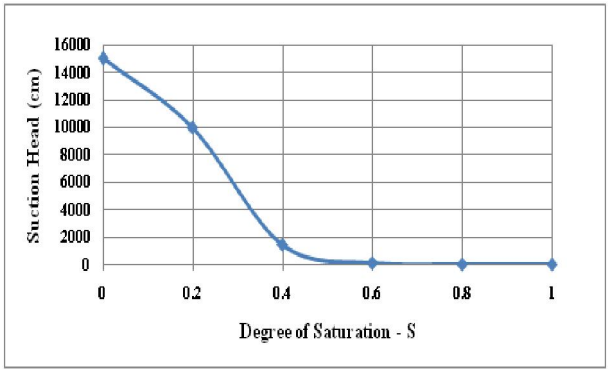

Figure (3): Soil water characteristic curve (pF curve) for a repacked loamy soil.

2) Green-Ampt Infiltration Model

Green and Ampt (1911) as reported by Hillel (1998) had developed another infiltration model (**Green-Ampt model**) that determines the infiltration rate.

If the bonding depth is negligible and the surface is thus maintained at a pressure head of zero, and incorporating gravity for vertical infiltration, **Green-Ampt** modelis as follows:

$$i = \frac{dI}{dt} = -K \frac{H_f}{L_f} = -K \frac{h_f - L_f}{L_f} \quad (9)$$

Where i is the infiltration rate, I is cumulative infiltration, h_f is actual suction at the wetting front, L_f is hydraulic pressure of water column above the wetting front, and ΔH_p is the pressure-head difference between the soil surface and the wetting front, which is obtained empirically. Assuming zero head at the soil surface, ΔH_p is then the suction head at the

wetting front. This equation suggests that the infiltration rate varies linearly with the reciprocal of the distance to the wetting front.

h_f was estimated empirically, to determine the infiltration rate of **Green-Ampt.**

In this work, instead of using empirical value for suction head at the wetting front, the infiltration rate is determined using Eagleson (1978) as in equation (4). Eagleson infiltration rate was incorporated in **Green-Ampt** model (equation 5) to determine suction head at the wetting front as:

$$h_f = L_f\left(1 - \frac{i}{K}\right) \quad \textbf{(10)}$$

Where h_f is the suction head at the wetting front, iis the infiltration rate, L_f is the depth of the wetting front and K is the saturated hydraulic conductivity.

Green-Ampt theory was found to apply particularly to infiltration into uniform, initially dry coarse-textured soils, which exhibit a sharp wetting front (Hillel and Gardner, 1970). The main assumptions of **Green and Ampt** approach are that there exists a distinct and precisely defined wetting front during infiltration. Although this wetting front moves progressively downwards as time proceeds, it is characterized by constant matrix suction at the wetting front, regardless of time and position. Furthermore, this approach assumes that, in the transmission zone behind the wetting front the soil is uniformly wet and of constant conductivity.

The wetting front is a plane separating a uniformly wetted infiltrated zone from a totally noninfiltrated zone. In effect, this supposes that the relation of hydraulic conductivity (K-h) versus suction head at the wetting front is discontinuous. The value of hydraulic conductivity prevailing at the wetting front changes abruptly from a high value, to a very much lower value.

These assumptions simplify the flow equation, making it amenable to analytical solution. Because a uniformly wetted zone is assumed to extend all the way to the wetting front, it follows that the cumulative infiltration I should be equal to the product of the wetting front depth L_f and the wetness increment $\Delta\Theta = \Theta_t - \Theta_i$ (where Θ_t is the transmission-zone wetness during infiltration and Θ_i is the initial profile wetness, which prevails beyond the wetting front).

Thus, the depth of the wetting front can be obtained as follows:

$$\mathbf{L_f} = \frac{I}{\Delta\boldsymbol{\theta}} \quad \textbf{(11)}$$

$\Delta\Theta$ is the difference in water content between the profile initial condition and saturation. Equation (11) determines the depth of the wetting front, knowing the cumulative infiltration and the initial moisture in the profile.

3. Results

Deep irrigation for maintaining higher moisture in the plant root zone

Frequent irrigation, once every 2 days with 2.5 mm depth of water, wets the surface 30 cm, which is completely lost by evaporation before the next irrigation as shown in figure (4). On the other hand, irrigation once every 2 weeks with 15 cm depth of water raises soil moisture at the depth of 60-100 cm below surface, which allows for better root growth, while the 30-60 cm depth maintains larger amount of moisture until next irrigation. Moisture near the surface (0-30 cm) fluctuates between larger-depth irrigations, and maintains more moisture as compared to center-pivot sprinkler irrigation.

Effects of magnetized saline irrigation water on moisture loss and salt leaching

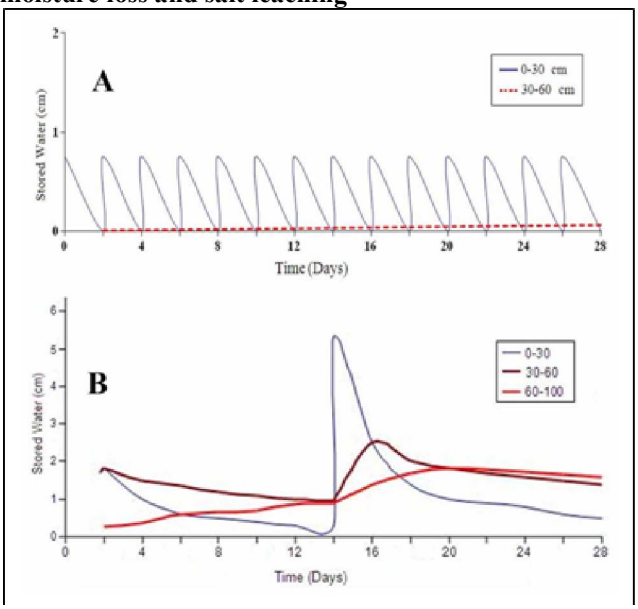

Figure (4). A) Moisture in the root zone in case of small-depth frequent irrigation (every two days). B) Moisture in the root zone in case of larger-depth less frequent irrigation (every two weeks) in a sandy loam soil.

Salinity analyses of leachates of soil pots are presented in Table (1). The first irrigation caused a leaching of 1.2 mg salts per magnetized pot as compared to 0.89 mg for normal pots, with a rate of increase in salt removal by magnetized water of about 35%. In the second irrigation the rate of increase of salt removal by magnetized water reached 48% as compared to normal water. Besides, the volume of leachates increased by 22% and 31% for the first and second irrigation with magnetized water.

The amount of retained moisture per pot was taken as a measure for soil holding capacity and was shown to decrease by magnetic treatment. On the

other hand, water retention in the second leachate was taken as a measure for evaporation loss during the previous drying cycle; evaporation loss according to this estimation was shown to decrease greatly by magnetic treatment.

Moreover salt retention per pot after the first irrigation was 10% greater in case of normal water compared to magnetized water. Such percentage exceeded 130% in the second irrigation. Thus, soil salinization could continue with a greater rate in the following irrigations with normal saline water as compared to magnetized water.

Table (1): Moisture and salt leached from soil pots as affected by magnetizing saline irrigation water (Hilal 2015).

Parameter	1st Irrigation		2nd irrigation		Total irrigations	
	Magnetized water	Normal water	Magnetized water	Normal water	Magnetized water	Normal water
Irrigation water						
Volume (cm^3)	**750**	**750**	**200**	**200**	**950**	**950**
Salt added (mg/ pot)	**4.36**	**4.36**	**1.14**	**1.14**	**5.5**	**5.5**
Drained water						
Volume (cm^3)	**142**	**116**	**135**	**103**	**277**	**219**
Salt Leached(mg/ pot)	**1.22**	**0.89**	**0.93**	**0.69**	**2.15**	**1.58**
Retained moisture	**608 cm^3**	**634 cm^3**	**65 cm^3**	**97 cm^3**	**-**	**-**
Retained salts	**3.14 mg**	**3.45 mg**	**0.21 mg**	**0.5 mg**	**3.35**	**3.95**

Effect of soil stratification on moisture retention and distribution in soil columns:

Sand/Sandy Loam (S/SL) columns retained higher moisture at the end of the drying period as compared to Sandy Loam/Sand (S/SL), homogeneous sand and homogeneous sandy loam columns. Experimental results in figure (5) show that the existence of sandy loam at the top of soil column resulted in a higher moisture loss by evaporation as the column retained only 190 g of moisture at the end of drying period, while sand if placed on column top greatly reduced evaporation and the column retained more than 400 g of moisture at the end of drying period.

Difference in behavior in different stratification cases is attributed to different unsaturated water suction heads that are lower in sand than that in sandy loam. Lower suction heads in sand at the surface result in weaker capillary movement which limits the effect of evaporation to little amounts of water near the soil surface, and increases downward flow of irrigation water.

On the other hand, when sandy loam is at the surface, stronger unsaturated water suction heads induce stronger capillary movement that extract deeper water from the surface sandy loam layer and result in higher evaporation losses. In case of sand at the surface followed by deeper sandy loam (fourth case), plant roots that grow mostly from 15 to 30 cm below the soil surface will extract its needs from the SL layer that is protected by the surface S layer with little evaporation losses.

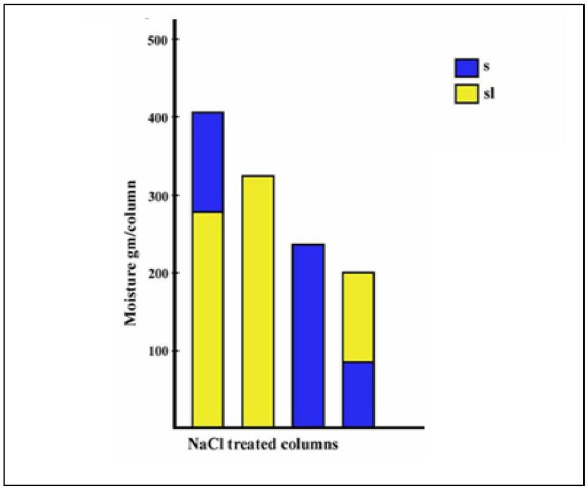

Figure (5): Effect of different stratifications of sand (S) and sandy loam (SL) soils on moisture retention in soil column after a period of one month drying.

Effect of Soil Stratification on Moisture and Salt Balance:

To control salt distribution in the root zone under saline conditions, the net effects of such parameters have been extensively studied in soil column experiments.

Data in table (2) represent moisture and salt distribution through 70 cm soil columns depth as affected by induced gravel layer of 5 cm thickness at depth of 25-30 cm, after 120 days of wetting and drying cycles, of 10 days intervals by 10,000 ppm NaCl solution.

The results revealed a positive effect of the induced gravel layer on moisture content in the layers

located above the gravel. The average increase of moisture content in the stratified columns reached 13% over that of the homogenous columns. Distribution in the entire soil columns is also shown in table (2). Salt concentration in layers, over the gravel, was reduced to distinctive degrees. Recorded EC values ranged between 2.3 to 4.5, dS/m, while they recorded 4.2 to 9.3 dS/m in homogenous columns.

Table (2). Effect of Soil Stratification on Moisture and Salt Distribution in Soil Columns,irrigated with 10.000 ppm NaCl Solution (after 120 days of wetting and drying cycles).

Depth of Soil Segment cm	Moisture Content % after 120 days of setting		EC of Soil Segment after 120 days of setting dS/m	
	Homogeneous	Stratified	Homogeneous	Stratified
0-5	5.5	5.8	9.3	4.5
5-10	6.5	7.1	3.1	1.7
10-15	6.7	7.6	3.3	1.7
15-20	7.1	9.2	3.7	1.9
20-25	8.5	11.5	4.2	2.3
25-30*	9.5	11.5	5.3	7.5
30-35	11.2	11.7	5.8	3.0
35-40	13.1	14.2	6.3	3.4
40-45	14.0	14.5	6.6	3.9
45-50	14.3	14.7	6.9	4.7
50-55	14.7	14.9	7.5	5.4
55-60	15.0	15.2	7.8	5.9
60-65	15.2	15.6	8.5	6.1
65-70	15.6	15.8	8.7	6.8

*Gravel layer of 5 cm thickness is placed at 25-30 cm depth.

Thus, an impeded gravel layer in sandy soil is expected to work as a trap for salts. The saline solution moves down ward through macropores into the gravel layer.

However, during the drying cycle, water moves upward partially in liquid form and partially in vapor, leaving at least part of the salt behind. Upon frequent wetting and drying cycles, salt concentration increases in gravel layer and decreases above and below it.

Path of water flow in macro and micro-pores during wetting:

Wild (1996) described downward water flow in non saturated soil column, as that water creeps over the solid particles from where the films are thickest to where they are thinner. This description is inconvenient. Water always flows in the path of least resistance, which leads to the flow mechanism described below.

The flow description adopted in this work is that during infiltration, water flows down in the soil profile in gravitational macropores, and is sucked into adjacent capillary micro-pores through the wet macropore walls. This makes downward water flow rate during ponded infiltration going by gravity above the field capacity, hydraulic conductivity value (-1/3rd to 0 atm.).Progressively, water is sucked into micropores by sorption suction head, which is lower than that already existing in micropores. Meanwhile, downward water flow during non-ponded infiltration goes by gravity at hydraulic conductivity rate between the field capacity and saturation.

This generates milder gradients of sorption suction head and hydraulic conductivity during sorption. This differs from Richards' Equation that assumes very steep suction head gradient between wet soil at the surface and dry soil below. According to Richards' Equation, downward water flow from wet to dry soil has very rapidly changed gradients which result in rapid changes in water contents. Thus, numerical solution of Richards' Equation encounters numerical instability problems that require a solution to use very small spatial and temporal increments.

Development of New Sorption Suction Head Curve

Considering the loamy soil given above that was used for determining the sorption suction head, and it has the pF curve shown in figure (4). The unsaturated hydraulic conductivity curve is determined by equation (8), while the Diffusivity is determined by trapezoidal rule graphical solution of equations (6,7).

Assuming an initially dry soil profile with Θ_o=0, the infiltration rate is determined by equation (8) and the wetting front depth is obtained using equation (11). Figure (6) shows infiltration rate (cm/hr), cumulative infiltration (cm), and the wetting front depth (cm) for an initially dry profile. Because of incorporating gravity head in equation (9), actual

suction at the wetting front is found to decrease after reaching a certain peak, as shown in figure (6). That suction head *'peak'* is considered the soil sorption suction head at the wetting front that raises the soil water content from Θ_o to Θ_s. Maximum wetting front suction head of 17.6 cm at 0.6 hr is highlighted.

Table (3) also shows the calculated infiltration rate (cm/hr), cumulative infiltration (cm) and depth of wetting front (cm), and suction of wetting front (cm) for an initially dry profile. Table (3) indicated that maximum suction head occurred at time 0.6 hours with the value of 17.61 cm. Infiltration rate ranged between 19 cm/hr at the first time step, and5 cm/hr at time 1.0 hr, with the value of 6.45 cm/hr at 0.6 hr where maximum suction head at the wetting front occurred. Infiltration rate indicates the antecedent water flow velocity entering the soil surface, while cumulative infiltration expresses the amount of water the entered the soil during the elapsed time. Depth of wetting front is calculated using equation (11). Suction at the wetting front, which is calculated by equation (10), increases to a maximum value of 17.6 cm at 0.6 hrs, and then decreases slightly to 17.0 cm at 1.0 hr. This maximum value is considered the sorption suction head for the initial water content of the profile (S=0 in this case).

Table (3).Calculated infiltration rate (cm/hr), cumulative infiltration (cm), depth of wetting front (cm) and suction of wetting front (cm) for an initially dry profile at Θ_o=0.

Time(hours)	Infiltration Rate (cm/hr)	Cumulative Infiltration(cm)	Depth of Wetting Front (cm)	Suction of Wetting Front (cm)
0	0	0	0	0
0.05	18.80	0.94	2.40	6.62
0.1	13.72	1.63	4.16	12.31
0.15	11.46	2.20	5.62	14.53
0.2	10.12	2.71	6.92	15.71
0.25	9.21	3.17	8.10	16.43
0.3	8.53	3.59	9.19	16.89
0.35	8.00	3.99	10.21	17.19
0.4	7.58	4.37	11.18	17.38
0.45	7.23	4.73	12.10	17.51
0.5	6.93	5.08	12.99	17.58
0.55	6.68	5.41	13.84	17.61
0.6	6.45	5.74	14.69	17.61
0.65	6.26	6.05	15.47	17.59
0.7	6.08	6.35	16.25	17.55
0.75	5.92	6.65	17.00	17.49
0.8	5.78	6.94	17.74	17.42
0.85	5.65	7.22	18.47	17.34
0.9	5.53	7.50	19.17	17.26
0.95	5.43	7.77	19.87	17.16
1	5.32	8.03	20.55	17.06

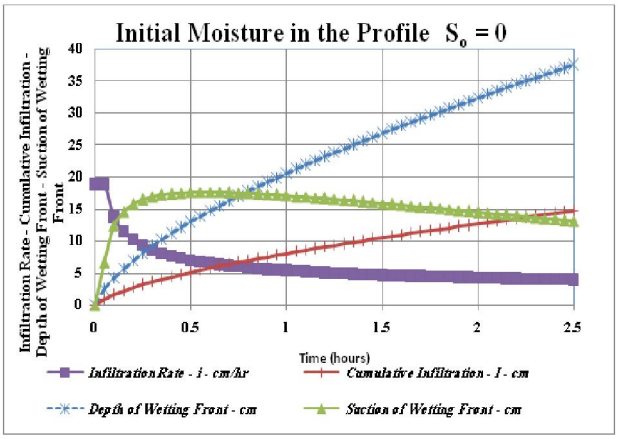

Figure (6): Calculated infiltration rate (cm/hr), cumulative infiltration (cm) and depth of wetting front (cm), and suction of wetting front (cm) for an initially dry profile at Θ_o=0.

Assuming different values of initial water content (S_o) in the profile, suction head at the wetting front is obtained for all values of initial water content in the profile. The resulting values that cover full range from initially dry soil (S=0) to initially saturated profile (S=1), are shown in Table (4). Maximum suction head occurring for each case is highlighted. Highest suction head at the wetting front varied from 17 cm at the initially dry profile, to about 11 cm for an initially wet profile.

Table (4) Suction at the wetting front for the illustrative example soil for different values of initial water content in the profile at increments of 0.1 S to cover the full range S= 0 to 1. Maximum value of wetting front suction head is highlighted which is considered the suction head (sorption).

TIME (hour)	Suction of Wetting Front for certain initial moisture content – cm									
	S_o= 0	S_o= 0.1	S_o= 0.2	S_o= 0.3	S_o= 0.4	S_o= 0.5	S_o= 0.6	S_o= 0.7	S_o= 0.8	S_o= 0.9
0	0	0	0	0	0	0	0	0	0	0
0.05	6.62	2.53	2.69	2.87	3.09	3.37	3.75	4.27	5.03	6.01
0.1	12.31	4.39	4.65	4.97	5.37	5.86	6.54	7.47	8.86	10.80
0.15	14.53	5.94	6.30	6.74	7.28	7.96	8.90	10.19	12.16	15.04
0.2	15.71	7.30	7.76	8.31	8.98	9.83	11.00	12.63	15.13	18.97
0.25	16.43	8.55	9.09	9.73	10.53	11.54	12.94	14.88	17.89	22.68
0.3	16.89	9.71	10.32	11.06	11.98	13.13	14.74	16.99	20.49	26.22
0.35	17.19	10.79	11.48	12.31	13.33	14.63	16.44	18.98	22.97	29.64
0.4	17.38	11.82	12.58	13.49	14.63	16.05	18.07	20.89	25.35	32.96
0.45	17.51	12.80	13.63	14.63	15.86	17.42	19.63	22.72	27.64	36.19
0.5	17.58	13.74	14.64	15.71	17.05	18.73	21.13	24.49	29.86	39.35
0.55	17.61	14.65	15.61	16.76	18.19	20.00	22.58	26.21	32.02	42.45
0.6	17.61	15.53	16.55	17.78	19.31	21.24	23.99	27.88	34.13	45.50
0.65	17.59	16.38	17.46	18.76	20.38	22.43	25.37	29.51	36.19	48.50
0.7	17.55	17.21	18.34	19.72	21.44	23.60	26.71	31.10	38.22	51.46
0.75	17.49	18.01	19.21	20.66	22.46	24.74	28.02	32.66	40.20	54.38
0.8	17.42	18.80	20.05	21.57	23.46	25.86	29.30	34.19	42.15	57.27
0.85	17.34	19.57	20.88	22.47	24.45	26.95	30.56	35.69	44.07	60.12
0.9	17.26	20.32	21.69	23.35	25.41	28.02	31.80	37.16	45.96	62.95
0.95	17.16	21.06	22.48	24.21	26.35	29.07	33.01	38.62	47.83	65.75
1	17.06	21.79	23.26	25.05	27.28	30.11	34.21	40.05	49.67	68.53

Figure (7) shows the trends of sorption suction heads at the wetting front for different values of the initial water content in the soil profile varying from dry (S=0) to saturation (S=1).In case of dry profile, suction head had sharp increase at the beginning of infiltration, followed by flat plateau. However, the plateau was followed by slight decline of wetting front suction head in case moderately wet initial profile. On the other hand, the initially wet profile had sharp increase in wetting front suction head at the beginning of infiltration, and declined fast to zero afterwards.

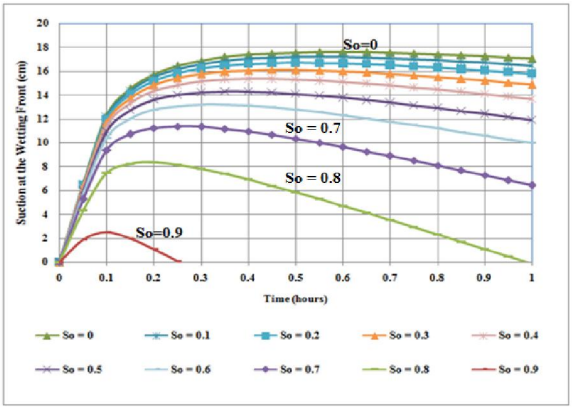

Figure (7): Suction at the wetting front for the illustrative example soil for different values of initial water content in the profile at increments of 0.1 S to cover the full range S= 0 to 1.

The 'peak' suction head value of each curve in figure (7) is considered the sorption suction head (cm), which is used to obtain the sorption suction head curve at all values of water content as shown in Figure (8).

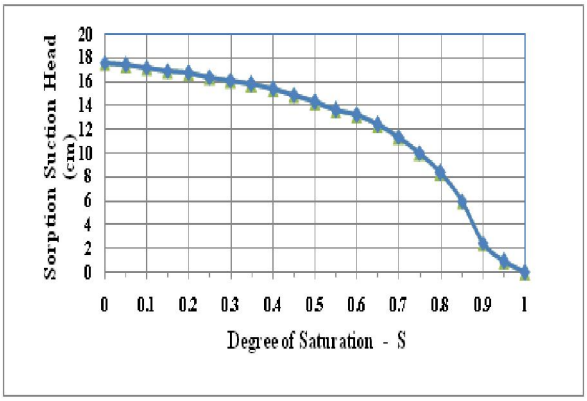

Figure (8). Calculated Sorption Suction Head (cm) that raises soil water from S_o to saturation.

Values in figure (8) obtained using methodology of this work are consistent with reported values for suction at wetting front in dry soil that varied from as low as 10 cm in sand, and up to 55 cm in fine clay (Brakensiek 1979; Brakensiek et al., 1980).

Deviation from Green and Amptas sumptions will require adjustment of the obtained curve in figure (8), when numerical solution of Richards' equation is

compared to observation (which will be done in future work). It is ***expected*** that, Adjusted Sorption Suction Head curve will run below the sorption suction head curve in figure (8), with significant drop above field capacity (field capacity is assumed in this work at 50% saturation).

Skaggs (1980) rewrote G&A as:

$$\boldsymbol{i = \frac{A}{I} + B} \qquad \textbf{(12)}$$

Where A and B are parameters that depend on the soil properties, initial water content and distribution, and surface conditions such as cover, crusting, etc. This equation assumed an average value for suction head at the wetting front. In addition to uniform soil profiles for which it was originally derived, Green and Ampt equation (9) was successfully applied for profiles that become denser with depth (Childs and Bybordi, 1969) and for soils with partially sealed surfaces (Hillel and Gardner, 1969), and for soils with non-uniform initial water contents (Bouwer, 1969). Green and Ampt equation (9) was also used to predict cumulative infiltration from steady rainfall into uniform soil with constant initial water contents (Mein and Larson, 1973). Smith (1972) and Reeves and Miller (1975) extended Green and Ampt as sumptions to unsteady rainfall rate that dropped below infiltration capacity for a period of time followed by a high intensity application. Skaggs (1980) applied rearranged Green and Amptequation (12) successfully to unsaturated profiles with shallow water tables with water contents in equilibrium with gravity.

Unsaturated Soil Moisture Movement during Sorption and Desorption

Moisture movement occurs below field capacity, where movement is by diffusion. Moisture movement doesn't necessarily carry salts with it.

When the soil is in sorption, downward water inflow into macropores of a soil segment is absorbed by the micropores and no downward outflow occurs until the micropores are filled. The limit of micropore water requirement is set empirically when the soil reaches field capacity (30%-60% of saturation; herein assumed at 50% saturation) after which downward gravitational water flow occurs. We use the continuity equation:

$$\boldsymbol{\frac{\partial \theta}{\partial t} = -\frac{\partial q}{\partial z}\ ;\ or\ \frac{\Delta \theta}{\Delta t} = q_{out} - q_{in}} \qquad \textbf{(13)}$$

Where Θ is volumetric soil water content (cm^3/cm^3), t is time (hours), z is vertical distance, q_{out} and q_{in} are out flux and influx (cm/hr), respectively. Downward influx into the soil will be expressed using Darcy's law as:

$$\boldsymbol{q_{downwards-in} = K(\theta_{sat})\frac{\partial H}{\partial z}}$$ under ponded infiltration **(14-a)**

and

$$\boldsymbol{q_{downwards-in} = K(\theta_{f.c})\frac{\partial H}{\partial z}}$$ under non- ponded infiltration **(14-b),**

and upward influx will be

$$\boldsymbol{q_{upwards-in} = K(\theta)\frac{\partial H}{\partial z}} \qquad \textbf{(15)}$$

where H = h-z, and h is the sorption suction head (shown in figure 8), and outflux from the soil during sorption will be:

$$\boldsymbol{q_{downwards-out} = 0\ if\ \theta < \theta_{f.c.}} \qquad \textbf{(16-a)}$$

and

$$\boldsymbol{q_{downwards-out} = K(\theta)\frac{\partial H}{\partial z}\ if\ \theta \geq \theta_{f.c.}} \qquad \textbf{(16-b)}$$

Thus, water movement in unsaturated soil during sorption will be solved using equations 13, 14 (a, b), 15 and 16 (a, b) using the adjusted sorption suction curve shown in figure (8). Meanwhile, unsaturated flow during redistribution occurs when water outflows from a soil segment that is in desorption, and inflows to another soil segment in sorption. Soil segment in desorption will follow the drying soil water characteristic curve of figure (3), and the other soil segment in sorption will follow the adjusted sorption curve of figure (8). When the two soil segments are in desorption, moisture movement will follow the equation

$$\boldsymbol{q_{in/out} = K(\theta)\frac{\partial H}{\partial z}} \qquad \textbf{(17)}$$

Where the drying (desorption) soil water characteristic curve (pF curve) of figure (3) is used for both soil segments and moisture will move from more moist soil to less moist soil.

Unsaturated Soil Moisture Profile during Ponded Infiltration

Consider the loamy soil profile with the properties shown above (figure 3 to figure 8), the profile is initially relatively dry at 20% saturation (at t=0: $S_{(z=0\ to\ z=100\ cm)} = 0.2$).Equations 13 to 17 are solved using the new sorption suction head curve for the case of ponded infiltration(at t > 0: $S_{(z=0)}=1.0$), where the soil surface is at saturation during one hour of infiltration. The lower boundary of the profile at z=100 cm is set as free gravitational flow ($q = K(\Theta)\ \partial H/\partial z$ for $\partial H/\partial z > 1$;and $q=0$ for $\partial H/\partial z < 1$).Solution of Equations 13 to 17that uses the new sorption suction head curve is done at relatively large fixed time step of 0.05hr (3 minutes), and fixed spatial increment of 5 cm. Figure (9) shows soil moisture profile during ponded infiltration every 0.25 hour (15 minutes), up to 0.75 hours, and compares it to solution of Richards' Equation simulated by program of Workman and Skaggs (1990).Simulation results of this work discharged more infiltration water entering into the profile that penetrated deeper as compared to Richards' Equation solution, as shown in figure (9).

Meanwhile, the wetting front of this work was a little milder than Richards' Equation.

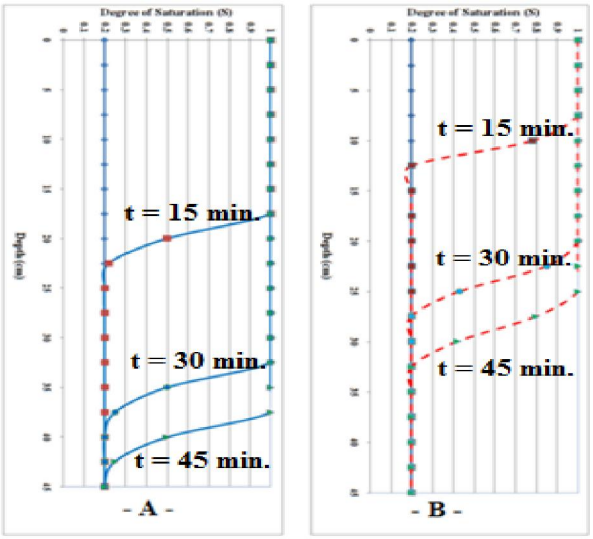

Figure (9). Comparison between (A) simulation of the developed model and (B) simulation of Richards' Equation solution of moisture content profile vs. depth after 15 min, 30 min and 45 min of infiltration into dry profile.

Unsaturated Soil Moisture Profile During Redistribution

Another case is simulated for redistribution of moisture in the soil profile 1.0 hour after the end of infiltration. The boundary condition at the soil surface is set as no flow boundary ($q = 0$ for $t \geq 0$). The lower boundary condition is set as free gravitational flow ($q = K(\Theta)\, \partial H/\partial z$ for $\partial H/\partial z > 1$; and $q = 0$ for $\partial H/\partial z < 1$). Moisture in the soil profile at zero time is the same for the two simulations. Figure (10) shows soil moisture content profile after one hour of redistribution following the end of ponded infiltration. Redistribution is a slower process where moisture is drained from macropores of the upper part of the profile and is absorbed by deeper soil segments. The upper part of the profile is in desorption, while the deeper part is in sorption. Gravitational flow that occurs above field capacity in the simulation of this work went faster than Richards' Equation solution. The drained water was absorbed deeper in the profile. More water was retained in the active root zone in the simulation of this work as compared to Richards' Equation solution (figure 10). Under the conditions of this study, the model of this work predicts better moisture conditions in the plant root zone for a variety of crops. Thus, the soil micropores absorb water from macropores until they reach field capacity, before allowing gravitational flow to carry water deeper in the profile.

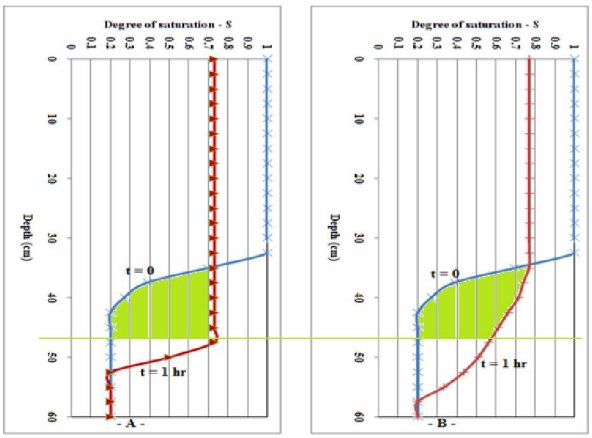

Figure (10). Comparison between (A) simulation of developed model and (B) simulation of Richards' Equation solution of moisture content profile vs. depth after 1.00 hr of redistribution following the initial condition at the end of irrigation.

References

1. Anwar, Nabil M. and Mostafa H. Hilal (2015). Benefaction of Saline water Irrigation in Desert Soils: II. Mathematical Modeling of the Distribution of Salts in Soil Macro and Micro-Pores during Wetting and Drying Cycles. Journal of American Science 2015;11(11): 12-23. (ISSN: 1545-1003) http://www.jofamericanscience.org
2. Bomba, S. J. (1968). Hysteresis and time-scale invariance in a glass-bead medium. Ph.D. Thesis, Univ. Wisconsin, Madison, WI.
3. Bouwer, H.(1969). Infiltration of water into non-uniform soil. J. Irrigation and Drainage Division, ASCE. 95(IR4):451-462.
4. Brakensiek, D.L.(1979). Comments on empirical equations for some soil hydraulic properties by R.C. Clapp and G.M. Hornberger. Water Resources Research, 15(4): 989-990.
5. Brakensiek, D.L., R.L. Engleman and W.J. Rawls (1980). Variation within texture classes of soil water parameters. ASAE paper No. 80-2006. Presented at the 1980 Summer ASAE meeting, San Antonio, TX, USA.
6. Childs, E. C. and M. Boyardi (1969). The vertical movement of water in stratified porous material - 1. Infiltration. Water Resour. Res., 5(2):446-459.
7. Crank, J. (1956). The Mathematics of Diffusion, Oxford University Press, New York, 1956.
8. Eagleson, Peter S. (1978). Climate, Soil and Vegetation: 3. A Simplified Model of Soil Moisture Movement in the Liquid Phase. Water Resour. Res., Vol. 14, 5: 722-730.
9. Elbana; Tamer A. (2013).Transport and adsorption-desorption of heavy metals in different soils. Ph.D. Dissertation, Louisiana State University; USA.
10. Green, W. H., and Ampt, G. A. (1911). Studies on soil physics: I. Flow of air and water through soils. J. Agr. Sci. 4, 1-24.

11. Haines, W. B. (1930).Studies in the physical properties of soils. V. Tile hysteresis effect in capillary properties and the modes of moisture distribution associated therewith. 20, 97-116.
12. Hilal,M.H. Abed F.H. and Bader M.A. (1997). Corrective Techniques for Soil and Irrigation Water Salinity in Desert Agro-Systems. The International Symposium on Sustainable Management of Salt Affected Soils in the Arid Ecosystem, 21-26 Sep., Cairo, Egypt. P. 320.
13. Hilal, M.H and Helal, M.M. (2000): Application of magnetic technologies in desert agriculture, II-Effect of magnetic treatments of irrigation water on salt distribution in olive and citrus fields and induced changes of ionic balance in soil and plant. Egyptian J. soil Sci. 40, No. 3, PP, 423-435.
14. Hilal, M.H. and Shata, S.M. (2000).Some aspects of moisture and solute transport in soils as affected by soil stratification and moisture content. Egypt. J, Appl. Science, 15, (7).
15. Hilal, M.H. (2015). Recent aspects for doubling wheat yield in Egypt. Publisher: Academic Bookshop; Cairo, Egypt. (In Arabic).
16. Hillel, D. and W.R. Gardner, (1969). Steady infiltration into crust topped profiles. Soil Science, 108: 137-142.
17. Hillel, D., and Gardner, W. R., (1970). Transient infiltration into crust-topped profiles. Soil Sci. 109, 69-76.
18. Hillel (1998). Environmental Soil Physics. Academic Press.
19. Jackson, Ray D. (1972).On the calculation of hydraulic conductivity. Soil Sci. Soc. Am. Proc. 36: 372-380.
20. Knuze, R.J., G. Uehara and K. Graham (1968). Factors important in the calculation of hydraulic conductivity. Soil Sci. Soc. Am. Proc. 32:760-765.
21. Mein, R.G. and C.L. Larson (1973). Modeling infiltration during a steady rain. Water Resources. Res., 9(2): 384-394.
22. Millington, R.J. and J. P. Quirk (1960). Permeability of porous soils. Transactions Faraday Society, 57:1200-1207.
23. Miller, E. E., and Miller, R. D.(1955a). Theory of capillary flow: 1. Practical implications. Soil Sci. Soc. Am. Proc. 19,267-271.
24. Miller, E. E., and Miller, R. D. (1955b). Theory of capillary flow: 2. Experimental information. Soil Sci. Soc. Am. Proc. 19, 271-275.
25. Miller, E. E., and Miller, R. D. (1956).Physical theory for capillary flow phenomena. J. Appl. Phys. 324-332.
26. Philip, J.R. (1960).General method of exact solution of the concentration-dependent diffusion equation. Aust. J. Phys., 13(1), 1-12.
27. Philip, J. R. (1964). Similarity hypothesis for capillary hysteresis in porous materials. J. Geophys. Res. 69, 1553-1562.
28. Philip, J.R. (1969). The theory of infiltration, in Advances in Hydrosciences, vol. 5, edited by V.T. Chow, pp. 215-296, Academic, New York.
29. Reeves, M. and E.E. Miller (1975). Estimating infiltration for erratic rainfall. Water Resour. Res. 11(1): 102-110.
30. Richards, L.A. (1931). Capillary conduction of liquid through porous medium. Journal of Physics, 1: 318–333.
31. Skaggs, R. W. (1980). Drainmod, Reference Report, Methods for Design and Evaluation of Drainage-Water Management Systems for Soils with High Water Tables; United States Department of Agriculture, Soil Conservation Service, South National Technical Center, Fort Worth, Texas, USA.
32. Smith, R.E.(1972). The infiltration envelope: Results from a theoretical infiltrometer. Journal of Hydrology, 17:1-21.
33. Szymkiewicz, Adam (2004). Modeling of Unsaturated Water Flow in Highly Heterogeneous Soils. PhD THESIS, Gda´nsk University of Technology, Poland.
34. Topp, G. C.; (1969). Soil water hysteresis measured in a sanely loam and compared with the hysteresis domain model. Soil Sci. Soc. Am. Proc. 33,645-651.
35. Topp, G. C., and Miller, F. E. (1966).Hysteresis moisture characteristics and hydraulic conductivities for glass-bead media. Soil Sci. Soc. Am. Proc. 30, 156-162.
36. *Takashinko*, y (1995). Indah Water Proposal. Non published tech. Report. Magnetic Tech. Dubai.
37. Van Genuchten, M. Th., Leij, F.J. and Yates, S.R. (1992), "The RETC Code for Quantifying the Hydraulic Functions of Unsaturated Soils," EPA/600S2-91/065.
38. Wild, Alan (1996). Soils and the environment. Cambridge University Press.
39. Workman, S. R., and Skaggs, R. W. (1990). Development and application of a Preferential flow model. Paper of American Society of Agricultural Engineers No. 90-2062 Summer Meeting, Columbus, Ohio.
40. Zhang, Hua and H. M. Selim (2005). Kinetics of arsenate adsorption-desorption in soils. Environ. Sci. Technol. 39:6101-6108.

5/25/2016